Journal of Materials and Engineering Structures

Research Paper

Studies on hardness and tensile testing of AlSi$_{10}$Mg produced by selective laser melting

Suresha S [a], Subramanya Raghavendra [b]

[a] *School of Mechanical Engineering, Reva University, Bangalore, India*

[b] *Department of Mechanical engineering, Sai Vidya Institute of Technology, Bangalore, India*

A R T I C L E   I N F O

A B S T R A C T

AlSi alloys have a wide range of applications in the Additive Manufacturing area, including automotive, aerospace, and residential industries. Despite their appealing mix of mechanical qualities, high heat conductivity, and low weight, they are more difficult to treat by Selective Laser Melting due to their high reflectivity and heat conductivity. In this work, samples were exposed to heat treatment at temperatures of 400°C, 500°C, and 550°C and an artificial ageing treatment for 180°C for 12h, to control the mechanical behaviour of selective-laser- melting (SLM)-produced AlSi10Mg alloys, after which material properties such as tensile strength and hardness were evaluated. The highest tensile and yield strengths are shown by the as-built SLM specimens, which have values of 432.45 and 322.76 MPa. On the other hand, the lowest tensile and yield strengths are shown by the solution heat-treated specimens, which have values of 168.11 and 90.52 MPa. Similar to as-built SLM specimens, the highest hardness value measured was 132.55Hv1.

1   Introduction

Product development and manufacturing technologies are all aimed at improving productivity by improving efficiency and product quality through the entire manufacturing process, from concept and detail design to quality control and packaging. Additive Manufacturing (AM) refers to a "process of joining materials to make objects from 3D model data, usually layer upon layer, as opposed to subtractive manufacturing methodologies". Its synonyms include: additive fabrication, additive processes, additive techniques, additive layer manufacturing. Selective laser melting (SLM) is an ALM process and emerged as a new manufacturing technique to directly fabricate metal alloys and metal matrix composites products. SLM, also termed Direct Metal Laser Sintering as similar to selective laser sintering (SLS), is one of the most versatile ALM processes to generate complex 3D parts by Solidifying successive layers of powder material on top of each other. Nowadays,

additive manufacturing (AM) has replaced some traditional metal manufacturing methods, such as melting and forging, in certain different production methods, notably in the aerospace and motor racing application industries. In real sense, the primary advantages, like the absence of manufacturing design constraints, shape freedom, high component complexity, combination of various parts onto a part, production of functionally graded materials, reduced tooling requirements, and the ability to produce on demand, were accomplished in all these application fields [1, 2].

Furthermore, it has recently been supported in the literature that SLM may be utilised to produce metal matrix composites (MMCs). This aim can be achieved in part by developing novel materials with greater qualities than those acquired through traditional techniques, and in part by improving the control, precision, and dependability of the SLM process [3, 4].

The method is characterised in that the metallic material in powder from is applied in the form of a metallic powder free of binders and fluxing agents, that it is heated by the laser beam to metallic powder free of binders and fluxing agents, that it is heated by the laser beam to metallic powder free of binders and fluxing agents, that it is heated by the laser beam to metallic powder is fully molten throughout at the point of impact of said laser beam. STL file which is the de-facto standard file format for additive manufacturing technologies. This file is then loaded into a file preparation software package for slicing the 3D data into layers, usually from 20μm to 100μm in thickness, creating a 2D image of each layer. After that, parameter, values and physical supports are assigned to allow the file to be interpreted and built by different types of additive manufacturing machines. The highly concentrated laser energy input in SLM results in large thermal gradients, which result in thermal stress in the part. Deformation, cracking, internal porosity and dimensional inaccuracy are four of the most common defects.

Characteristics of the material, especially those that control the thermal response of materials, such as melting temperature, transformation temperatures, thermal conductivity, specific heat capacity, thermal diffusivity, coefficient of thermal expansion, flow properties, laser absorption, latent heat of vaporization, and etc., originate from chemical composition and are the major parameters to select the appropriate method and parameters of powder bed laser processing. These properties affect crack sensitivity, porosity, heat affected zone (HAZ) embrittlement, poor absorption of the radiation, etc [5]. Due to its excellent mechanical characteristics, such as hardness and strength, in the heat treated form, Al–Si–Mg alloys are now in high demand for a variety of applications, including motor racing, the automobile sector, and aerospace and heat exchanger systems. These alloys have typically been utilised for lightweight and thin-walled casting parts, as well as components with complicated geometry that are subjected to high stresses [6]. Many investigations have been conducted on these alloys, ranging from the initial powders through the potential end uses of lightweight lattice structures [7, 8].

But at the other hand, there are not many studies that focus on investigating how changes in energy affect the microstructure properties of the AlSi10Mg alloy produced by SLM Speed up the scan [9]. It is well known that the AlSi10Mg alloy part produced by SLM's processing could base on precise microstructure. Further research into how heat treatment and artificial ageing affect the evolution of microstructure during SLM will be interesting and valuable.
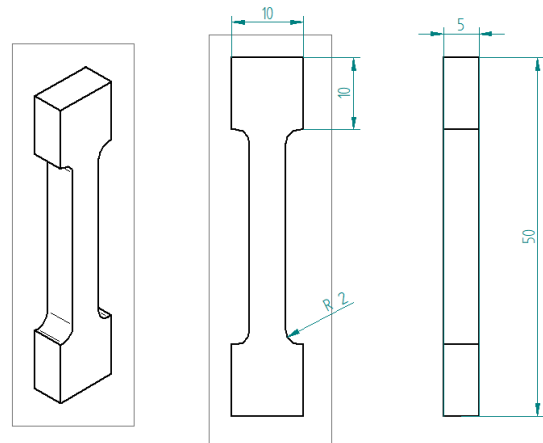
Understanding microstructure control and the quality of SLM-fabricated parts requires extensive research into how heat treatment and artificial ageing affect materials that have undergone SLM processing. The purpose of this study is to investigate Influence of heat treated and artificial aging on the microstructure and mechanical properties of SLM-produced AlSi10Mg alloy parts.

2   Methodology

A gas atomized AlSi10Mg powder with a normally distribution from 20 μm to 63 μm. AlSi10Mg tensile bars shown (Figure 3.2) & Figure 3.3) shows the 2D and 3D view of the specimen; were fabricated on a EOSINT M 280. The SLM machine is equipped with a 400W Gaussian beam fiber laser with a focal laser beam diameter of 80 μm. The processing parameters have been optimized as follows: the laser power was 350W, laser scan speed was 1140 mm/s, the powder layer thickness was 50μm and the scan spacing was 170μm. The SLM production was performed in an inert argon atmosphere to avoid the pick-up of interstitial oxygen (lower than 0.2%). The AlSi10Mg parts were cut from the Al substrate using wire electrical discharge machining after production, it is worth nothing that the substrate was heated to 100°C for the purpose of reducing internal stress during the SLM process.
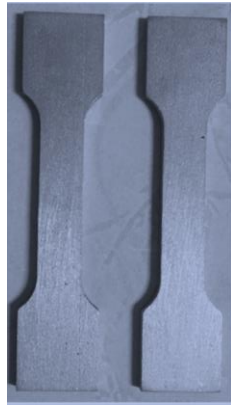
Fig. 1 – Tensile specimens of AlSi10Mg alloy made by SLM   *Fig. 2 – Dimension of the specimen in mm*

In accordance with the standard T6 heat treatment process, the SLM-produced AlSi10Mg specimens were solution-treated at the different temperatures of 450°C, 500°C, and 550°C for 2h, followed by water quenching, after the solution heat treatment, one half of the specimens were immediately subjected to artificial aging at 180°C for 12h, and then all the samples were equally water quenched to room temperature.

Table 1 – Material Composition in (%wt)

Si	Fe	Cu	Mn	Mg	Ni	Zn	Pb	Sn	Ti
10	0.55	0.05	0.45	0.3	0.05	0.1	0.05	0.05	0.15

The tensile strength of the AlSi10Mg specimens before and after the heat treatments was characterized by a high precision electronic universal testing machine AG-100kN, Shimadzu with a constant strain rate of 1mm/min. The tensile specimen is illustrated in figure 1. Vickers hardness tests were carried out on a 430SVD hardness test machine at a load of 1000 gf and a loading time of 15s.

3 Mechanical properties

The tensile stress-strain curves obtained from the room temperature tensile testing on the as-built and different solution heat-treated AlSi10Mg specimens are shown in Figure 4.1. The variations of the tensile strength, yield strength and ductility with the solution temperature are given in Figure 4.3. The as-built SLM specimens exhibits the highest tensile and yield strengths of (432.45 MPa and 322.76 MPa), respectively, but possesses a lower ductility of 5.2%. The solution heat treatment has a great influence on the mechanical properties of the SLM made AlSi10Mg specimens. As the sample is solution heat-treated at 450°C for 2 h, there is a dramatically decrease in both tensile and yield strengths (282.36 MPa and 196.58 MPa, respectively), whist a large increase in ductility of (13.4%) can be observed. With further increase of the temperature up to 500oC, the tensile and yield strengths are reduced to (234.75 MPa and 126.00 MPa) respectively, and the ductility increases to (23.5%). However, when the temperature reaches 550oC, the specimens exhibit the lowest tensile and yield strengths (168.11 MPa and 90.52 MPa, respectively), while the ductility slightly increases to the maximum (23.7%). For the specimens subjected to both heat treatment and artificial aging at 180°C for 12 h, the mechanical properties are shown in Figure 4.3. it can be found that the ultimate strength and ductility both decrease with the increase in the temperature. The tensile strength decreases from 197.11 MPa to 187.14 MPa, while the ductility decreases from 23.3 to 19.5, as the solution temperature increased from 500°C to 550°C.

The high strength of the as-built SLM AlSi10Mg specimens can be attributed to the grain refinement. The effect of grain size on the mechanical properties can be rationalized by the semi-empirical Hall-Petch (HP) relationship, which is indicated in Eq. (1):

$$\sigma = \sigma_o + kd^{-\left(\frac{1}{2}\right)}$$

(1)

Where σ is the proof stress, σo is the friction stress for dislocation movement, k is the Hall-Petch coefficient, and d is the grain size. The size-induced strengthening results from the pile-up of dislocations at grain boundaries as well as resistance of the dislocation to slip transfer. Grain size refinement leads to reduction of the distance between the Si particles, which can give a considerable contribution to the strength because the increased Al-Si interface can effectively reduce the movement of dislocations [10], moreover, due to the nano-sized eutectic network Si in the as-built AlSi10Mg sample, the localized shear stress can be relived and hence increase the strength.
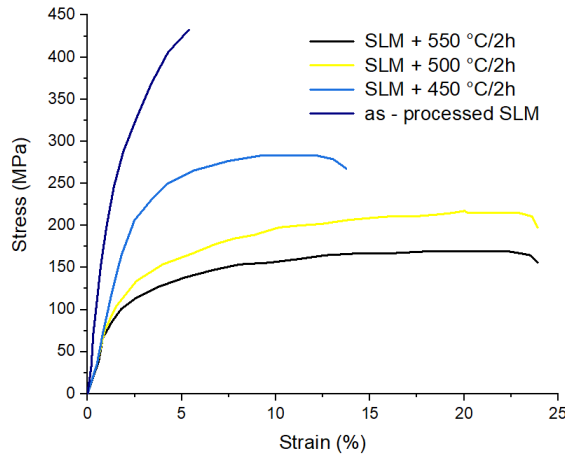
Fig. 3 – Room temperature tensile stress-strain curves of the as-built SLM samples that solution heat-treated at different temperature
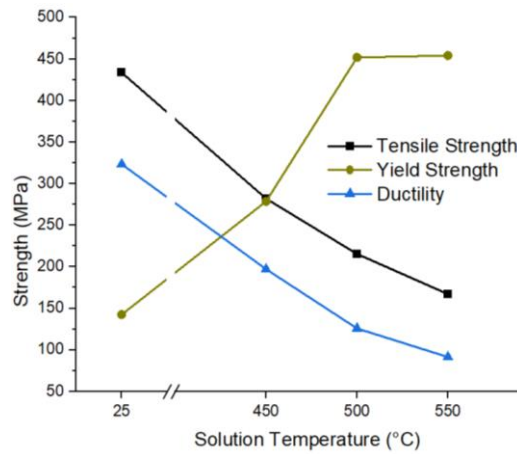

*Fig. 4 – Corresponding mechanical data*

The strength and ductility after heat treatment are influenced by many factors, such as number, morphology and size of the Si phase, initial hardening rate and recovery rate. The last two factors are closely related to the solute content in the solid solution. Upon solution and artificial aging, the Si atoms trapped in the Al matrix are rapidly precipitated out onto the existing eutectic network Si, thus reducing the solid solution strengthening. Meanwhile, the distance between the Si particles increases significantly, which also contributes to the decreased of tensile and yield strengths. As to the ductility of the as-built SLM samples and solution heat-treated specimens in this study, two aspects need to be considered. Firstly, the decrease in the number of Si particles and increase in size induce the reduction of localized stress or strain. Secondly, solution heat treatment reduces the residual stresses that are built up during the SLM process. These two aspects benefit the enhancement of the ductility of the solution heat-treated AlSi10Mg specimens.

Vickers micro-hardness is introduced and the corresponding results are illustrated in Figure 4.4. In general, the hardness values of the heat-treated specimens are lower than those of the as-built ones. Due to the fine dispersion of eutectic Si in the Al matrix, the as-built AlSi10Mg SLM specimens have the maximum micro-hardness value, namely 132.55 Hv1. After the solution treatment at 450 °C for 2 h, a significant decrease in micro-hardness can be observed (95.65Hv1). When the solution

treatment temperature is further increased from 500 °C to 550 °C, the micro-hardness decreases from approximately 87.85 Hv1 to 63.55 Hv1. It is worth noting that artificial aging also has a negative effect on the micro-hardness of the samples that have been subjected to the solution treatment. After the artificial aging at 180 °C for 12 h, the micro-hardness further reduces to 78.15 Hv1, 60.55 Hv1 and 52.5 Hv1 for the specimens that have been solution heat-treated at 450 °C, 500 °C and 550 °C, respectively, as illustrated in the red bars in Figure 4.4. This behaviour is in a good agreement with the evidence found in the tensile tests. This result can be also attributed to the coalescence of small Si particles as well as Ostwald ripening, which result in an increase in size and decrease in the number of particles.
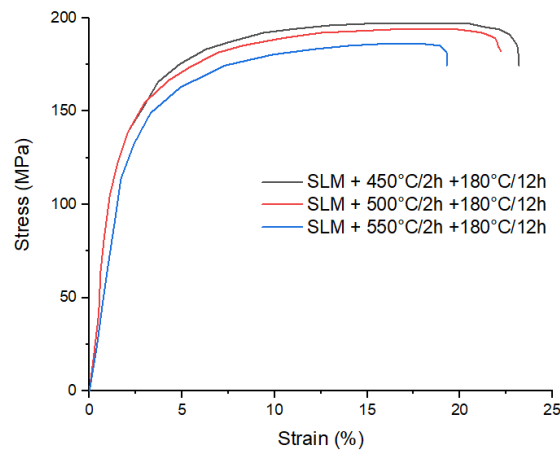
Fig. 5 – *Tensile test Stress-Strain curves of the solution + artificial aging specimens*
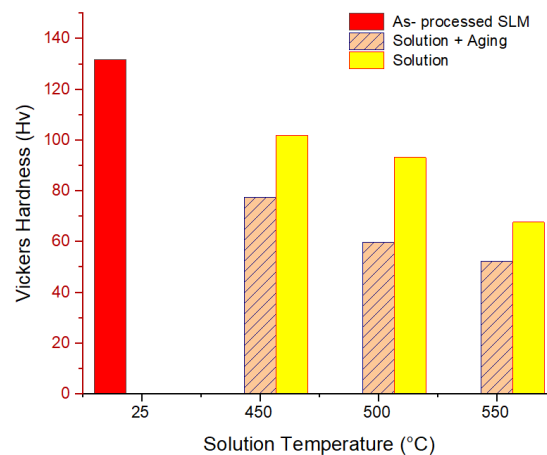
Fig. 6 – *The Vickers Hardness of the as- built and Heat-Treated SLM specimens*

It is well known that the microstructure of AlSi10Mg alloy can be influenced by superheating. The underlying reason had been attributed to the existence of two typical temperatures, usually donated by the dissolution temperature Td and the branching temperature Tb. At the temperature below Td, the Al and Si-rich particles which have been inherited from the solid AlSi10Mg alloy exist in the liquid phase. Once the temperature exceeds Td, these particles begin to be melted [11]. When the temperature is over Tb, molten Al and Si can be considered to mix homogenously. According to previous studies, Td and Tb of Al- Si10Mg alloy should be around 1020 °C and 1170 °C, respectively which are much higher than the eutectic temperature of Al-Si alloys (577 °C). During the SLM process, the temperature of a large part of the melt track exceeds Td but does not reach Tb. In addition, the short interaction time between laser and material, and the formation of liquid oscillations or capillary waves intensify the inhomogeneous microstructure. This could be due to the fast melting/solidification induce thermal accumulation and residual stresses to form during the SLM process [12]. Therefore, an inhomogeneous Al-rich and Si-rich microstructure is expected, which is helpful to form heterogeneous nucleation and enhance the nucleation rate. Due to the extremely high cooling rate (about 106 °C/s) of SLM, the above mentioned inhomogeneous microstructure will retain in the Al matrix. During the solidification process, the Si phase with higher melting

point firstly precipitates and grows up in the form of particles most likely by a heterogeneous nucleation mechanism. Then, with the decrease in temperature, the α-Al phase then nucleates and grows in the Si depleted zone around the Si particles, which inhibits the growth of the Si particles [13]. The continuous growth of the α-Al phase results in an increased Si concentration in the residual liquid. As the concentration of Si increases to a certain extent, the liquid phase may transform into the eutectic zone eventually resulting in the cooperative growth mechanism between Si and Al, and then yielding the eutectic phase in the latter stages of solidification. A very steep temperature gradient occurs on the surface of the melted track due to the high laser energy density and heat conductivity of Al. The large temperature gradient induces a highly undercooling condition, leading to the fibrous morphology of the Si crystals. Therefore, a microstructure with fibrous Si network distributed in supersaturated Al matrix forms in the SLM-processed AlSi10Mg alloy. Temperature gradient in SLM process influence on micro-segregation, phases formations and grain structures of the specimen [14].

Table 2 – Result of Tensile test and Hardness test

Types of Heat Treatment	Yield Strength (MPa)	Ultimate Tensile Strength (MPa)	% elongation of Ductility	Vickers Hardness (Hv_1)	Artificial Aging (ST +180ºC/12h)		
					Ultimate Strength (MPa)	Ductility (%)	Vickers Hardness (Hv_1)
As Received	432.45	322.17	5.3	132.55	_	_	_
ST 450ºC/2h	282.36	196.58	13.4	95.65	198.87	23.8	78.15
ST 500ºC/2h	234.75	126.00	23.5	87.85	197.11	23.3	60.55
ST 550ºC/2h	168.11	90.52	23.7	63.55	187.14	19.5	52.5
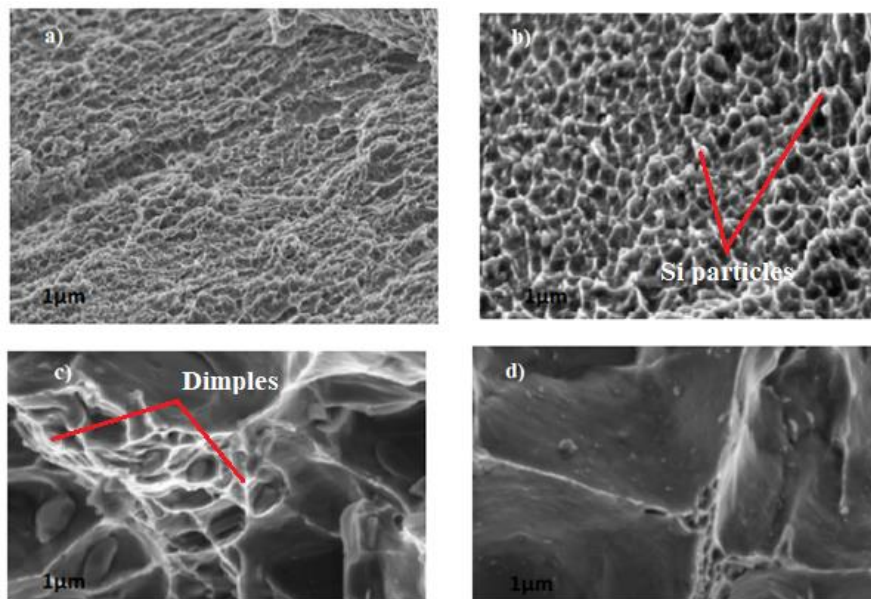
Fig. 7 – SEM images of the fracture surfaces of the SLM AlSi10Mg parts with the different heat treatment conditions a) as Processed b) Heat treated at 450ºC, c), Heat Treated 500°C and d) Heat treated at 550ºC.

The fibrous Si phases in the as-built SLM samples are extremely fine (200–300 nm), which results in a large total interfacial energy γAl/Si between Al and Si phases [15]. In addition, other kinetics or thermodynamic factors include the wettability (normally ex- pressed by the contact angle θc) and the local concentration of Al and Si atoms. These phenomena provide a high original driving force for the Si atoms coarsening. With the increase in heat treatment temperature, the increased original driving force gives rise to the precipitation of a significant amount of Si from the Al matrix. The availability of the precipitated Si may thus provide an additional contribution to the driving force for the growth of the Si particles. Moreover, when heat-treated at a high temperature, Si phase undergoes a thermally activated growth process. This enables the growth of Si phase along with the lowest free energy direction.

Figure 7a-7d illustrates the fracture surface areas of the developed samples and heat-treated tensile specimens. Due to uniaxial tension, the pores formed by the SLM process were opened. The evident cleavage-fracture structure was caused by the SLM process's residual stress and fine anisotropic columnar grains. The cleavage structure also resulted in relatively brittle fracturing.

In comparison to the samples as-fabricated, the heat treatment aided grain growth, Si precipitation, and residual stress release, all of which contributed to the formation of a more uniform microstructure. It is noted that the dimples in the heat-treated samples were larger than those in the samples that were manufactured, which could also be attributed to the fact that the heat treatment caused the grains to grow. By eliminating heat affect zones (HAZ), this one as microstructure is improved by favouring the sphereodization of interdendritic eutectic Si particles and decreasing the crack initiation. The nearby fine dimple regions, which are characterised by ductile fractures, are different from the central smooth area, which signifies a fragile rupture region. Large pores, which initiated fractures during the tensile test, turned into the preferred locations for inhomogeneous deformation at high stress levels, which led to the beginning of cracking.

4 Conclusions

In this study, the effects of the solution and artificial aging heat treatments on the phase, mechanical properties of the SLM-produced AlSi10Mg specimens are systematically studied. The main results and findings are as follows.

The as-received SLM parts were very brittle because of the residual stress developed during the processing.

The solutionized sample was much softer than the as received sample. Hence we can conclude that the residual stresses developed during processing were relieved from the solutionizing heat treatment.

As the solutionizing temperature was decreasing the strength & hardness found to be decreasing. Hence from our studies we can conclude that depending on the ductility required we have to choose the solutionizing temperature.

The variation in size of Si particles has a significant influence on the mechanical properties of the AlSi10Mg specimens. The tensile strength decreases from 434.25 MPa for the as-built specimens to 168.11 MPa for the specimens that solution heat-treated at 550 °C for 2 h. in contrast, the fracture strain remarkably increases from 5.3% to 23.7%.

To summarise all of the findings and observations, it should be highlighted that SLM technology provides a wide range of possibilities for manufacturing complex-shape structures and components. However, in order to achieve high mechanical properties and a favourable microstructure, ageing temperature and time will influence porosity, grain refinement, and changes in dislocations of the materials. Solution heat treatment lowers residual stresses that are built up during the SLM process. These factors contribute to the increased ductility of solution heat-treated AlSi10Mg specimens.

It is worth noting that artificial ageing has a negative impact on the micro-hardness of solution-treated samples. Because of the fine distribution of eutectic Si in the Al matrix.

REFERENCES

[1]- S. Mellor, L. Hao, D. Zhang, Additive manufacturing: A framework for implementation. International Journal of Production Economics, 149 (2014) 194-201. doi:10.1016/j.ijpe.2013.07.008.

[2]- S. Ford, M. Despeisse, Additive manufacturing and sustainability: an exploratory study of the advantages and challenges. Journal of Cleaner Production, 137 (2016) 1573-1587. doi:10.1016/j.jclepro.2016.04.150.

[3]- S. Kumar, J.P. Kruth, Composites by rapid prototyping technology. Materials & Design, 31(2) (2010) 850-856. doi:10.1016/j.matdes.2009.07.045.

[4]- T.B. Sercombe, X. Li, Selective laser melting of aluminium and aluminium metal matrix composites: review.

Materials Technology, 31(2) (2016) 77-85. doi:10.1179/1753555715Y.0000000078.

[5]- N.D. Alexopoulos, S.G. Pantelakis, Quality evaluation of A357 cast aluminum alloy specimens subjected to different artificial aging treatment. Materials & Design, 25(5) (2004) 419-430. doi:10.1016/j.matdes.2003.11.007.

[6]- T. Kimura, T. Nakamoto, Microstructures and mechanical properties of A356 (AlSi7Mg0.3) aluminum alloy fabricated by selective laser melting. Materials & Design, 89 (2016) 1294-1301. doi:10.1016/j.matdes.2015.10.065.

[7]- D. Buchbinder, W. Meiners, K. Wissenbach, R. Poprawe, Selective laser melting of aluminum die-cast alloy— Correlations between process parameters, solidification conditions, and resulting mechanical properties. Journal of Laser Applications, 27(S2) (2015). doi:10.2351/1.4906389.

[8]- N. Read, W. Wang, K. Essa, M.M. Attallah, Selective laser melting of AlSi10Mg alloy: Process optimisation and mechanical properties development. Materials & Design (1980-2015), 65 (2015) 417-424. doi:10.1016/j.matdes.2014.09.044.

[9]- X. Teng, G. Zhang, J. Liang, H. Li, Q. Liu, Y. Cui, T. Cui, L. Jiang, Parameter optimization and microhardness experiment of AlSi10Mg alloy prepared by selective laser melting. Materials Research Express, 6(8) (2019) 086592. doi:10.1088/2053-1591/ab18d0.

[10]- X.P. Li, X.J. Wang, M. Saunders, A. Suvorova, L.C. Zhang, Y.J. Liu, M.H. Fang, Z.H. Huang, T.B. Sercombe, A selective laser melting and solution heat treatment refined Al–12Si alloy with a controllable ultrafine eutectic microstructure and 25% tensile ductility. Acta Materialia, 95 (2015) 74-82. doi:10.1016/j.actamat.2015.05.017.

[11]- P. Yuan, D. Gu, D. Dai, Particulate migration behavior and its mechanism during selective laser melting of TiC reinforced Al matrix nanocomposites. Materials & Design, 82 (2015) 46-55. doi:10.1016/j.matdes.2015.05.041.

[12]- L. Zhou, T. Yuan, R. Li, J. Tang, G. Wang, K. Guo, Selective laser melting of pure tantalum: Densification, microstructure and mechanical behaviors. Materials Science and Engineering: A, 707 (2017) 443-451. doi:10.1016/j.msea.2017.09.083.

[13]- L. Xi, P. Wang, K.G. Prashanth, H. Li, H.V. Prykhodko, S. Scudino, I. Kaban, Effect of TiB2 particles on microstructure and crystallographic texture of Al-12Si fabricated by selective laser melting. Journal of Alloys and Compounds, 786 (2019) 551-556. doi:10.1016/j.jallcom.2019.01.327.

[14]- A. Mostafaei, R. Ghiaasiaan, I.T. Ho, S. Strayer, K.-C. Chang, N. Shamsaei, S. Shao, S. Paul, A.-C. Yeh, S. Tin, A.C. To, Additive manufacturing of nickel-based superalloys: A state-of-the-art review on process-structure-defect-property relationship. Progress in Materials Science, 136 (2023) 101108. doi:10.1016/j.pmatsci.2023.101108.

[15]- P. Ashwath, M.A. Xavior, A. Batako, P. Jeyapandiarajan, J. Joel, Selective laser melting of Al–Si–10Mg alloy: microstructural studies and mechanical properties assessment. Journal of Materials Research and Technology, 17 (2022) 2249-2258. doi:10.1016/j.jmrt.2022.01.135.